PROCEEDINGS, 41st Workshop on Geothermal Reservoir Engineering
Stanford University, Stanford, California, February 22-24, 2016
SGP-TR-209

Preliminary Simulations of Carbon Dioxide Injection and Geophysical Monitoring to Improve Imaging and Characterization of Faults and Fractures at EGS Sites

Curtis M. Oldenburg[1], Thomas M. Daley[1], Andrea Borgia[1], Rui Zhang[2],

Christine Doughty[1], T.S. Ramakrishnan[3], Bilgin Altundas[3], Nikita Chugunov[3]

[1]Energy Geosciences Division 74-316C, Lawrence Berkeley National Laboratory, Berkeley, CA 94720

[2]University of Louisiana at Lafayette, Lafayette, LA

[3]Schlumberger-Doll Research, Cambridge, MA

cmoldenburg@lbl.gov, tmdaley@lbl.gov, aborgia@lbl.gov, rxz1961@louisiana.edu, cadoughty@lbl.gov, ramakrishnan@slb.com, baltundas@slb.com, nchugunov@slb.com

Keywords: EGS, CO_2, Faults, Fractures, Characterization, Active seismic monitoring

ABSTRACT

Faults and fractures filled with hot brine are difficult to image and characterize at EGS sites because they are practically indistinguishable from surrounding matrix heterogeneity using traditional seismic and well-logging tools. We are investigating the use of CO_2 injection and production (push-pull) for contrast enhancement of faults and fractures for better characterization by active seismic and wireline well-logging approaches. In addition, we are modeling the pressure- and flow-rate-transient response of the system during push-pull to augment geophysical fault and fracture characterization. The approach consists of numerical simulation and feasibility assessment using conceptual models typical of EGS sites. Faults and fractures in the deep subsurface tend to occur in zones and sets with associated damage and gouge regions that are parallel to the slip plane(s) and that provide a larger volume for uptake of CO_2 than the volume provided by the slip plane(s) alone. CO_2 injected for push-pull well testing has a preference for flowing in the fault and fracture zone rather than entering the matrix because supercritical CO_2 is non-wetting relative to water and the permeability of open fractures and fault gouge is much higher than matrix. Numerical flow simulations using TOUGH2/ECO2N show that the CO_2 is driven upward by buoyancy in the slip plane during the push cycle over day-long time scales, but also flows into the gouge and damage zones on either side of the slip plane where upward flow due to buoyancy is smaller because of lower permeability. Recovery of CO_2 from the slip plane region during the pull cycle is limited because of buoyancy effects. Numerical modeling of elastic wave propagation in a system with discrete fractures was carried out using anisotropic finite difference codes from SPICE with modifications for fracture compliance. We modeled surface and vertical seismic profile (VSP) configurations of time-lapse active-source seismic monitoring with 5% added noise. Results suggest that for a 10 m-thick zone consisting of ten fractures each with 1 mm aperture slip plane, CO_2 can be best imaged using time-lapse differencing of the P-wave and P-to-S-wave scattering in a VSP configuration. Wireline well-logging tools that measure electrical conductivity show some promise as another means to detect and image the CO_2-filled fracture near the injection well and potential monitoring well(s), especially if a saline-water pre-flush is carried out to enhance conductivity contrast. These multiple complementary characterization approaches will be integrated in iTOUGH2 to carry out joint inversion to develop working models of fault and fracture zone characteristics relevant to EGS energy recovery at prototypical sites.

1. INTRODUCTION

Faults and fractures, either natural or a result of stimulation, are needed to provide permeability for sustainable geothermal energy production from high-temperature liquid dominated geothermal systems in crystalline rocks. But one or two large fractures or faults may dominate fluid production and thereby provide poor thermal sweep through the geothermal resource. Shown in Figure 1 are four different end-member configurations of fractures that could be encountered in the natural state or after stimulation to create an Enhanced Geothermal System (EGS). The fracture pattern and properties shown in Figure 1a may provide a sustainable geothermal fluid production, while those in Figures 1b-d may be controlled by just one or two fractures and lead to inefficient and unsustainable extraction of thermal energy from the resource. In the cases where one major fault or large fracture dominates the flow, stimulation may be needed to create a more pervasive network of fractures to access the entire volume of hot rock.

In order to design fracture stimulation or to evaluate existing fractures and faults in high-temperature EGS reservoirs, effective fracture and fault characterization is needed for both the natural and stimulated faults and fractures. In this paper, we describe our progress in evaluating the use of CO_2 injection into faults and fractures as a way of improving EGS reservoir characterization. The idea is that CO_2 injected into faults and fractures will create a larger contrast for active seismic and well-logging imaging, while also providing a pressure-transient response; from these data we hope to characterize the fracture or fault system. Our approach to developing and testing this idea is based on modeling and simulation of the integration of a suite of monitoring approaches that could be applied to a push-pull injection of CO_2 into faults or fractures. The approach begins with simulation of the push-pull injection of CO_2 into a generic fault or fracture and modeling of the hydraulic pressure-transient analysis. Next we will simulate active seismic monitoring of the CO_2-filled fractures or faults along with wireline well-logging approaches. These hydraulic and geophysical monitoring data will ultimately be inverted to derive likely configurations and properties of the fault or fracture system.

In this brief paper, we provide a report on our progress in the areas of defining the model system, simulations of CO_2 injection, simulations of active seismic modeling for imaging fractures filled with CO_2, and evaluating which wireline well-logging tools might be capable of imaging fractures or faults with variable CO_2 saturation in high-temperature systems. Future conference papers will summarize progress in the pressure-transient and coupled inversion of the full suite of (simulated) observations.

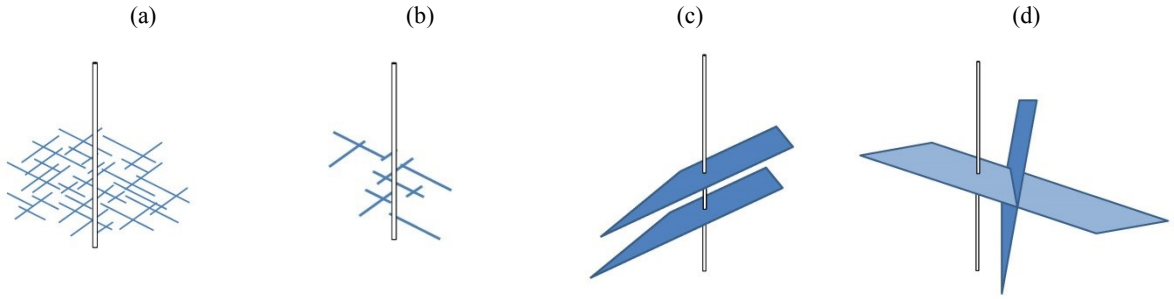

Figure 1. Idealized end-member fracture configurations around a vertical well: (a) dense fracture network; (b) sparse fracture network; (c) discrete non-communicating dominant fractures; and (d) discrete communicating dominant fractures.

2. GENERIC MODEL SYSTEM

Many potential EGS sites are in extensional tectonic environments and have poorly connected vertical faults and fractures (e.g., Faulds et al., 2010; Lutz et al., 2009; Genter et al. 2010), a configuration we call topology X (or Y) because the faults and fractures tend generally to be perpendicular to the horizontal (X- or Y-axis). We have adopted parallel vertical fractures and faults as the generic model system for our preliminary demonstration of the CO_2 push-pull characterization approach. Slip along a vertical fault plane usually produces a complex fault structure containing up-to-many-meter-thick fault gouge, one or more slip-planes within the gouge, and a damage zone outside the fault gouge characterized by tensional cracks extending into unfractured rock (the matrix). The relevant properties of fault and fracture sets are the size, shape, aperture, roughness, orientation relative to gravity, gouge thickness, damage-zone thickness, density of secondary fractures, tension shears), and the fracture spacing. These features are shown in Figure 2a along with our model conceptualization and nomenclature (Figure 2b). While fractures lack a gouge zone, for the purposes of the push-pull characterization approach presented here, faults and fractures are lumped together and our approach is applicable to better characterization of either faults or fractures or both.

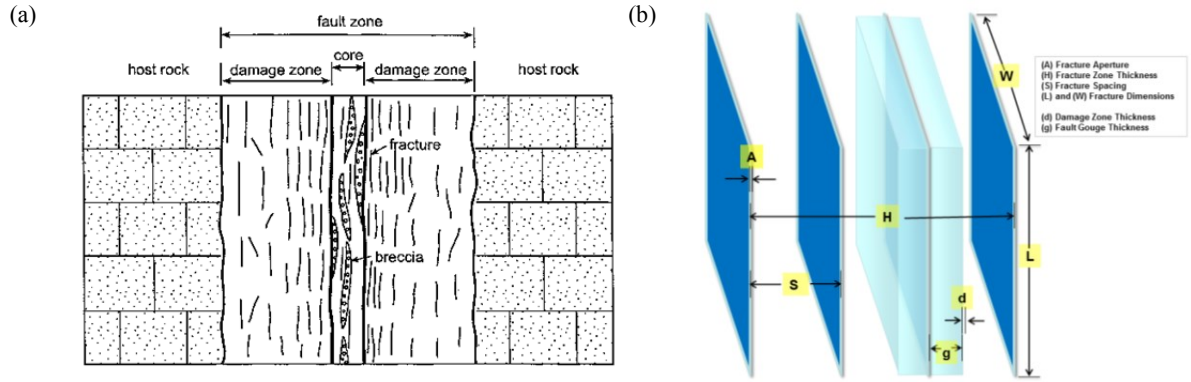

Figure 2. (a) Conceptual model of fault zone from Gudmundsson et al. (2002), along with (b) our model system terminology of a fracture and fracture set.

3. SIMULATION OF CO_2 INJECTION AND PRODUCTION

The flow and transport properties of CO_2 relevant to its use in brightening faults and fractures for active seismic or well-logging imaging are (1) CO_2 is much more compressible than water at EGS conditions, creating a large P-wave velocity contrast (note that the lower relative density of CO_2 is a second order effect on compressional velocity), (2) CO_2 is non-wetting and will therefore tend to stay in the fault/fracture and resist flowing into fine-grained matrix, and (3) CO_2 is less dense and less viscous than ambient brine at geothermal conditions. Although $scCO_2$ has gas-like viscosity which enhances its mobility, it is quite dense relative to other gases like nitrogen which is an advantage for decreasing buoyant rise in vertical faults and fractures to facilitate producing CO_2 back (the pull part of push-pull).

Simulations of the push-pull injection-production of CO_2 are carried out using TOUGH2/ECO2N (Pruess et al., 2012; Pan et al., 2014) in an idealized fault or fracture. The model domain for simulating CO_2 push-pull is shown in Figure 3 with model dimensions and the symmetry of the system (which allows us to model only one-quarter of the full system). We use a discretization with grid blocks of size

20 m × y × 20 m, where y = 10^{-4} m in the slip-plane, and 10^{-3}, 10^{-2}, 10^{-1}, and ~1 m in the fault gouge, 10^{-1} m in the damage zone, and ~1 m, and ~10 m in the matrix. The fracture is assumed to be between 2-3 km depth with geothermal gradient of 40 °C/km, fully saturated by brine with salt mass fraction equal to 0.1 at hydrostatic pressure. The boundary condition is closed to fluid flow on the top and open to fluid flow on the sides and bottom. Additional numerical simulation parameters are given in Table 1.

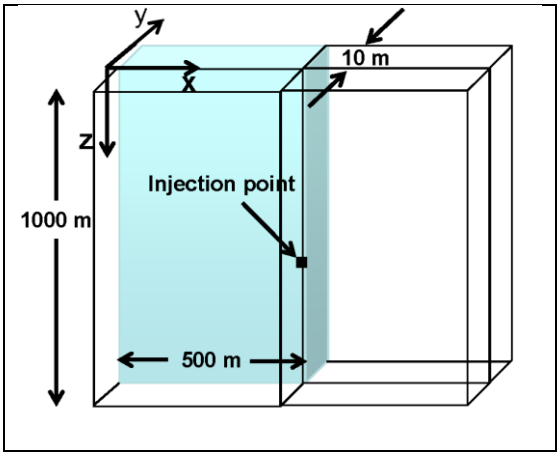

Figure 3. Model domain for push-pull simulations. Because of symmetry, we only model one-quarter of the actual system.

Table 1. Model parameters for push-pull simulations

Zone	Thickness (m)	Porosity (vol %)	Per-mea-bility (m^2)	Rock grain density (kg m^{-3})	Rock grain specific heat (J/(kg°C)	Thermal cond.[1] (W/(m°C))	Pore com-press-ibility. (Pa^{-1})	Capillary pressure (Pa)	Relative permeability
Slip plane	10^{-4}	0.5	10^{-12}	2700	1000	2.51	7.25 x 10^{-12}	none	Corey S_{lr} = 0.3; S_{gr} = 0.05
Fault gouge	1	0.1	10^{-13}	2700	1000	2.51	7.25 x 10^{-12}	VanGenuchten[3] λ = 0.4438; S_{lr} = 0.0, $1/P_0$ = 2.402e-4 Pa^{-1}; P_{max} = 1.e8 Pa; S_{ls} = 1.0;	Corey* S_{lr} = 0.3; S_{gr} = 0.05
Damage zone	10^{-1}	0.05	10^{-14}	2700	1000	2.51	7.25 x 10^{-12}	VanGenuchten[3] λ = 0.4438; S_{lr} = 0.0, $1/P_0$ = 2.402e-4 Pa^{-1}; P_{max} = 1.e8 Pa; S_{ls} = 1.0;	Corey S_{lr} = 0.3; S_{gr} = 0.05
Matrix	10	0.01	10^{-16}	2700	1000	2.51	7.25 x 10^{-12}	VanGenuchten[3] λ = 0.4438; S_{lr} = 0.0, $1/P_0$ = 1.485e-6 Pa^{-1}; P_{max} = 1.e8 Pa; S_{ls} = 1.0;	Corey S_{lr} = 0.3; S_{gr} = 0.05

[1]under liquid-saturated conditions. [2]Corey (1954); [3]Van Genuchten (1980)

Results of preliminary simulations showing pressure and CO_2 saturation are shown in Figures 4-6 for ten days of injection (push) with a 2 MPa overpressure, and one day of production (pull) with a 4 MPa underpressure relative to initial hydrostatic pressure. As shown in Figure 5, a large CO_2 plume is formed in the slip plane, and this CO_2 moves upward by buoyancy. Despite the relatively high density of CO_2 relative to other gases, the large contrast relative to native brine causes upward movement that makes it difficult to produce the CO_2 back during the pull phase. The inability to produce all of the CO_2 back does not compromise the overall geophysical characterization because we can use differencing of the seismic and well-logging data between the pre- and post-CO_2 injection periods. Figure 6 shows the CO_2 saturation in the gouge, in which the CO_2 forms a smaller plume with lower saturation, but this plume is thicker than the plume in the slip plane and therefore potentially creates a greater contrast for geophysical monitoring.

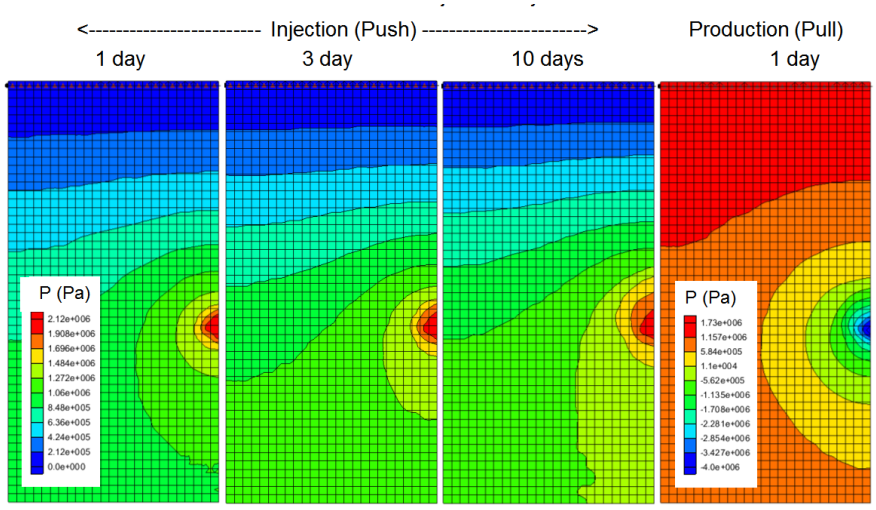

Figure 4. Pressure in the slip plane for closed top boundary case.

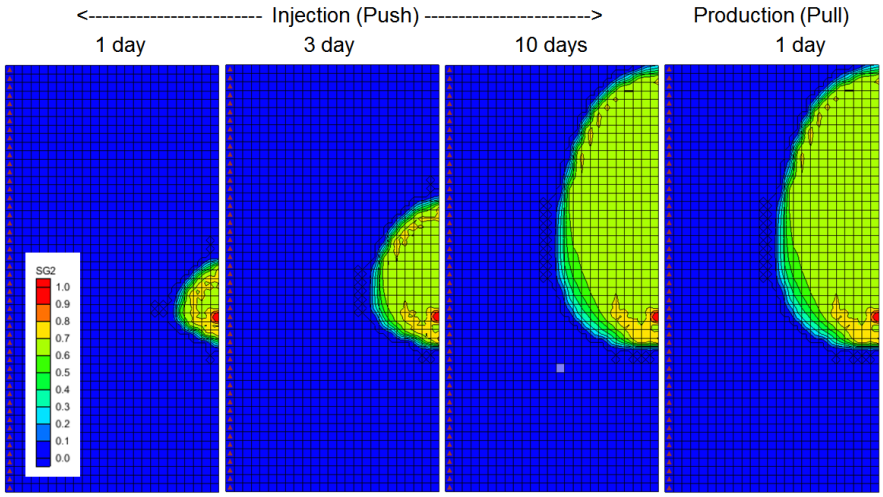

Figure 5. CO_2 saturation in the slip plane showing buoyant rise of CO_2. Buoyancy makes it difficult to produce the CO_2 back during the pull phase.

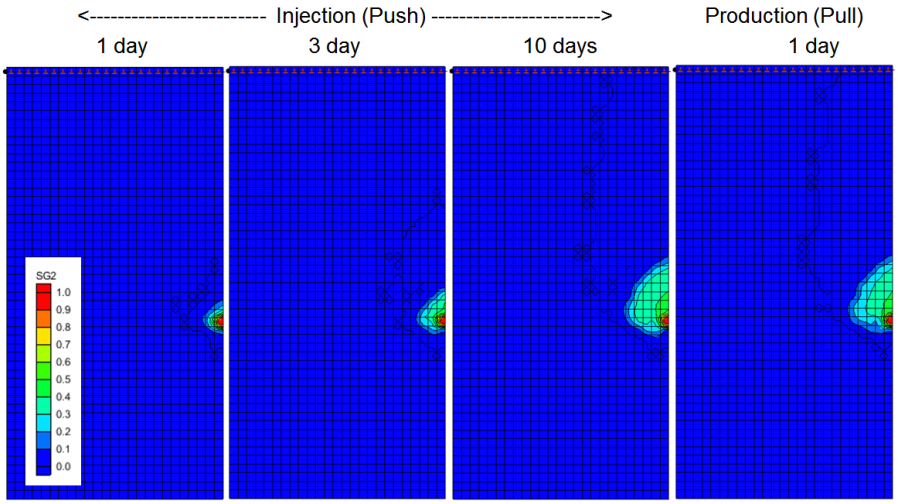

Figure 6: CO_2 saturation in the gouge showing smaller saturation than in the slip plane but still significant for property contrast especially considering the larger thickness of the gouge relative to slip plane.

4. SIMULATION OF ACTIVE SEISMIC MONITORING

In this effort we simulate active seismic monitoring to address the question of whether CO_2 injected into faults and fractures can enhance detectability by active seismic approaches, and if so, can active seismic methods be used to characterize the fault or fracture zone? At the heart of this question is whether the CO_2 makes enough contrast over enough volume to affect seismic wave propagation at a level that is resolvable. Our approach is to simulate active seismic imaging using finite difference solutions to wave propagation equations as implemented in a code originally from SPICE (http://www.spice-rtn.org/library/software.1.html) but which has been modified at LBNL for parallel processing, different boundary conditions, and for consideration of fracture properties. The approach uses a discrete grid with explicit finite-difference technique introduced by Madariaga (1976), Virieux and Madariaga (1982), Virieux (1986a). A perfect match layer (PML) boundary condition is used to reduce undesirable edge effects (Roden and Gedney, 2000, Komatitsch and Martin, 2007, Martin et al., 2008a,b, Martin and Komatitsch, 2009). For 3D calculations, an MPI (Snir et al., 1998) approach is implemented to improve computational efficiency. The inclusion of fractures follows the method of Coates and Schoenberg (1995) using a fracture compliance approach to anisotropic modeling. The change in fracture compliance for CO_2 displacing brine is calculated using the method of Nakagawa and Schoenberg (2007).

For testing the capability of active seismic monitoring to detect and characterize faults and fractures, we chose a hypothetical fracture system consisting of ten vertical fractures 500 m in vertical extent and spaced 1 m apart. Fracture properties are shown in Table 2. The fracture zone creates an anisotropic region in the isotropic background. The temperature was set at 200 °C, pressure 20 MPa, and salinity 1×10^5 ppm. The monitoring configuration is shown in Figure 7 with source placed 2 km offset from the fracture zone which is at a depth of 1800 m. Receivers are assumed to be in a borehole 50 m from the fracture zone. We added 5% noise to the simulation of seismic wave propagation in the system in surface and Vertical Seismic Profiling (VSP) monitoring configurations. Differencing of results from the pre-CO_2 injection to the post-CO_2 injection allows very small changes in seismic signal characteristics to be detected.

Table 2. Prototypical rock and fluid properties for preliminary active seismic modeling.

Matrix properties	**Values**	**Fracture properties**	**Values**
Porosity	20%	Porosity	50%
		Fracture width	0.1 cm
Solid bulk modulus	43.5 GPa	Fracture permeability	0.5×10^{-12} m^2
Fluid bulk modulus	2.25 GPa		
Frame bulk modulus	20.9 GPa	Dry normal compliance	1×10^{-11} m/Pa
Frame shear modulus	15.6 GPa	Shear compliance	3×10^{-11} m/Pa
Solid density	2650 kg/m^3	Solid density	2650 kg/m^3
Fluid density	Varying	Fluid density	Varying
Fluid viscosity	Varying	Fluid viscosity	Varying

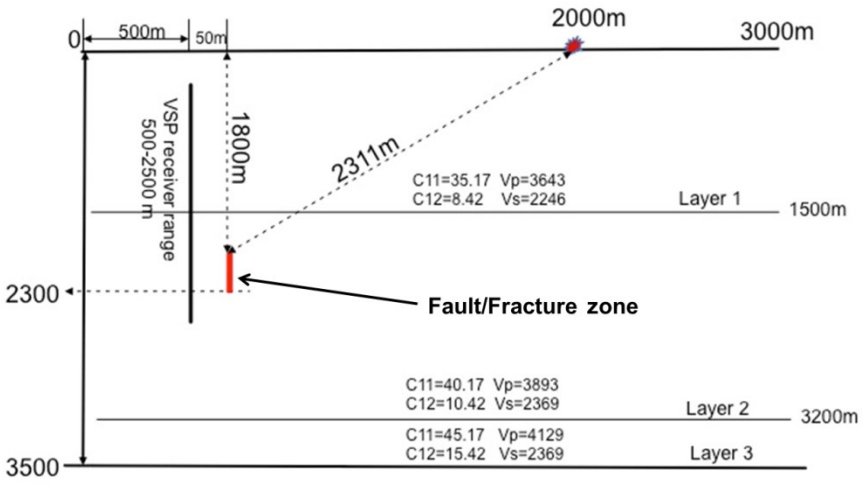

Figure 7. Conceptual model for simulating active seismic imaging of a fault/fracture zone (red) consisting of ten fractures spaced 1 m apart with fracture planes 500 m on a side. Anisotropic elastic constants and isotropic background velocities are shown for each layer.

As shown in Figure 8, the simulated vertical component of the surface seismic shot gather shows increased P-P and P-S scattering occurring in the 50% CO_2-saturated fractures. Strong S-S scattering (not shown) was observed in the horizontal component. However the 5% noise level nearly obscures the observed difference. Greater sensitivity to CO_2 saturation in the fracture zone was observed for seismic monitoring in the Vertical Seismic Profiling (VSP) configuration as shown in Figure 9 for the vertical component. Similar increased sensitivity was observed for the horizontal component. These preliminary results suggest that the VSP method would be preferable to characterize a vertical fault/fracture zone 10 m wide at EGS conditions.

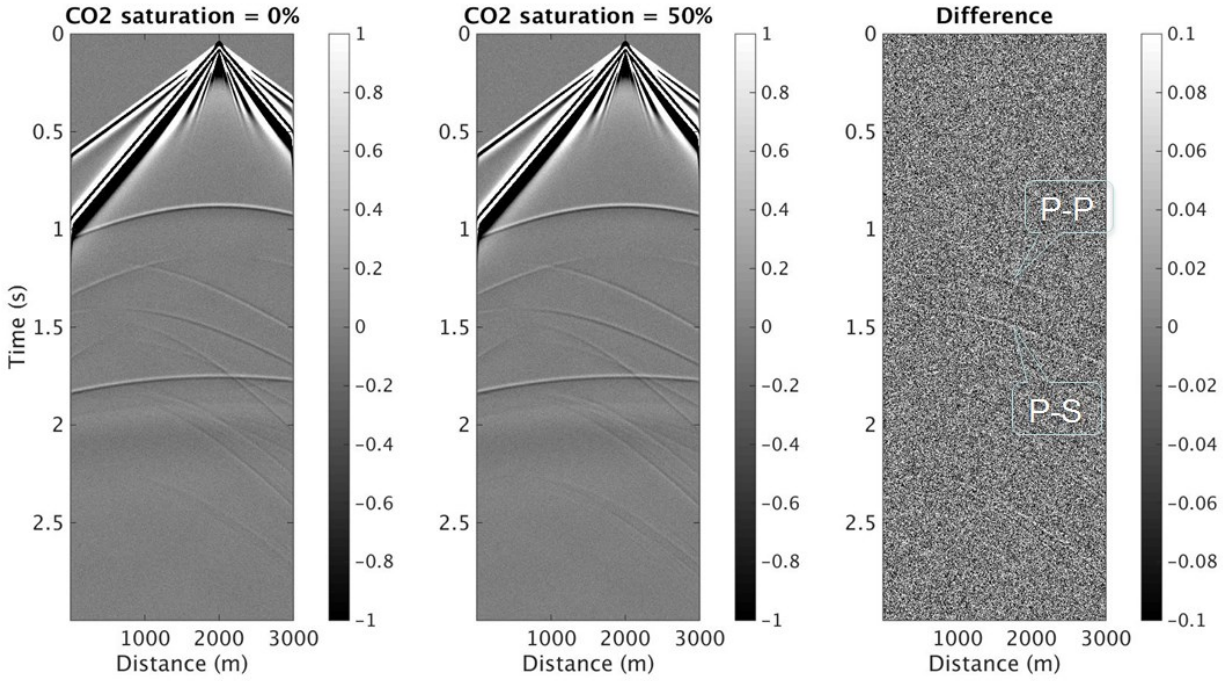

Figure 8: Vertical component of surface seismic shot gather shows increased P-P and P-S scattering from 50% CO_2-filled fracture zone.

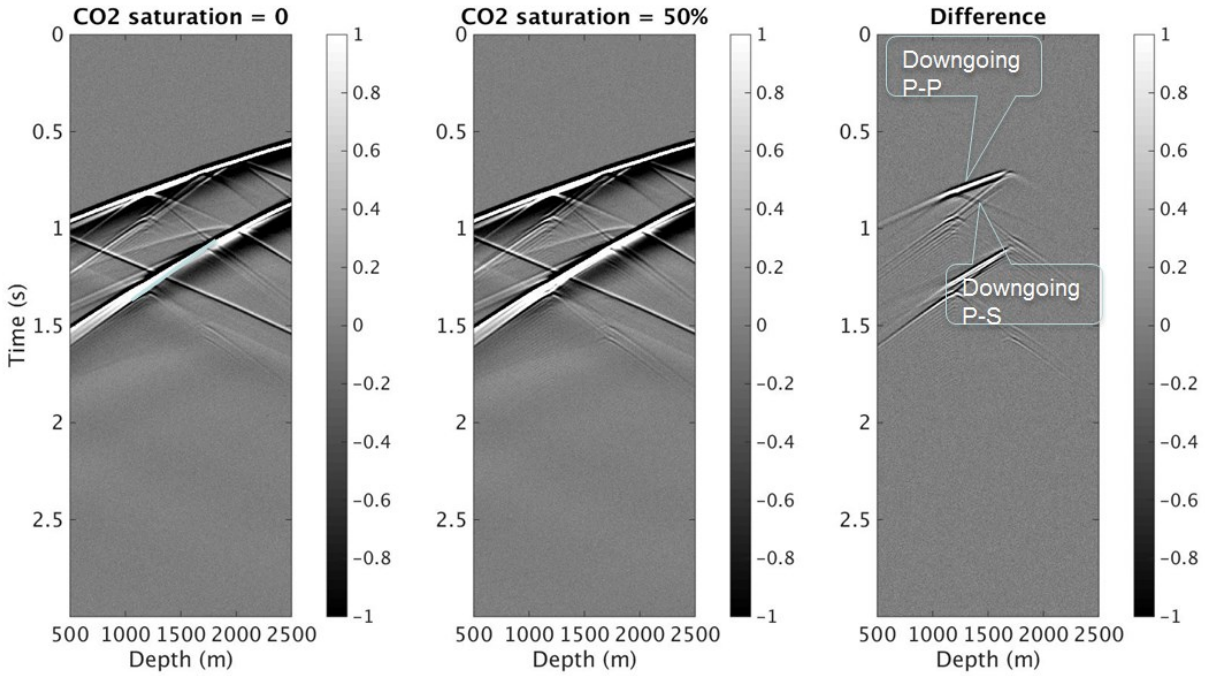

Figure 9: Vertical Seismic Profile (VSP) acquisition geometry has greater sensitivity than surface gathers as shown here by the change in vertical component (note the scale of the right-hand panel is 10 times that in Figure 8).

5. FEASIBILITY SCOPING OF WELL-LOGGING METHODS

Well logging can be used as another approach to detect and characterize CO_2-filled faults and fractures. The high-temperature of EGS sites (T > 175 °C) limits the number tools available for wireline well logging, and requires use of so-called "hostile environment" versions of the tools. In this preliminary effort, we have used simple methods to estimate the likelihood of various existing high-temperature well-logging approaches to be effective. The approaches we investigated are shown in Figure 10 along with preliminary estimates of sensitivity of the measurement of the effective property to various expected ranges of properties (saturation, salinity, ΔP, and ΔT). As shown, the tools are expected to be sensitive to saturation, and to lesser degree, salinity. None of the tools is expected to be sensitive to ΔP or ΔT.

The next step in evaluating well-logging approaches is to consider the actual geometry of a vertical fault or fracture with a given aperture and saturation of CO_2 and determine if the effective property change will be detectable in that particular geometry in the rock. For these estimates, the porosity is used as a proxy for fracture aperture, with small values (e.g., 0.01) representing small apertures. We used simple mixing models, Gassmann model, and Archie's law to estimate changes expected in effective properties across the various regions of a fault zone or fracture at geothermal reservoir conditions. The results of this analysis are summarized in Figure 11 which shows that only the changes in electrical conductivity and neutron capture cross section in the gouge zone are expected to be potentially distinguishable from matrix following CO_2 injection. The reason for this is that the slip plane has small aperture whereas the gouge zone is much larger.

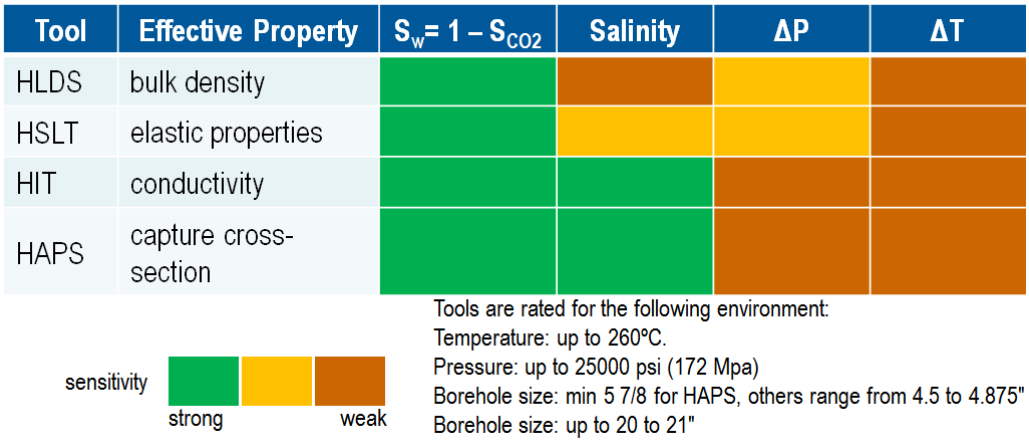

Figure 10: Wireline well-logging tools showing estimated feasibility based on the computed dynamic range for effective properties (bulk density, elastic properties, conductivity, and capture cross section) for expected ranges of $S_w = 1 - S_{CO2}$, salinity, *P*, and *T*. HLDS = Hostile Environment Litho-Density Sonde; HSLT = Hostile Sonic Logging Tool; HIT = Hostile environment Induction imager Tool; HAPS = Hostile Accelerator Porosity Sonde.

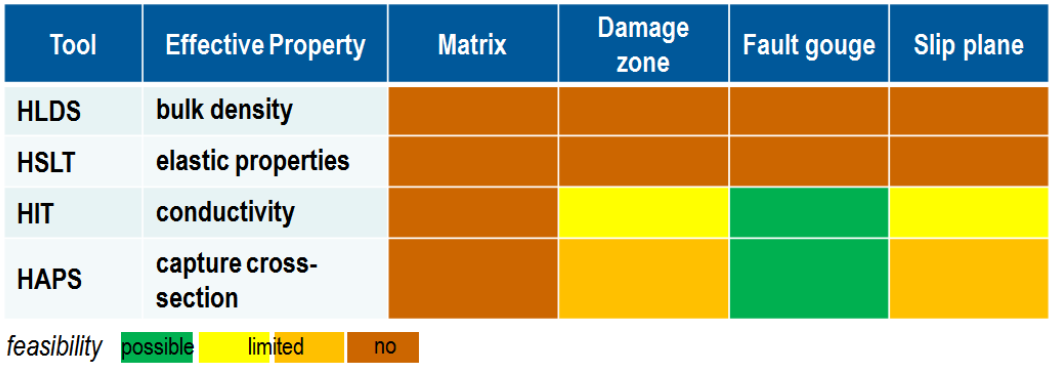

Figure 11: Wireline well-logging tools showing estimated feasibility for measuring changes in effective properties in the four regions of the fault or fracture zone (matrix, damage zone, fault gouge, and slip plane) based on realistic assumed dimensions of the regions. Only in the fault gouge are the conductivity and capture cross-section property changes expected to be large enough for use in distinguishing CO_2 from background brine. HLDS = Hostile Environment Litho-Density Sonde; HSLT = Hostile Sonic Logging Tool; HIT = Hostile environment Induction imager Tool; HAPS = Hostile Accelerator Porosity Sonde.

6. CONCLUSIONS

We are simulating an integrated CO_2 push-pull, pressure transient, active-seismic and well-logging monitoring approach aimed at better characterization of natural and stimulated faults and fractures at EGS sites. Our simulations to date show that CO_2 injected into slip-plane results in saturations over 50% as CO_2 spreads laterally and vertically. Buoyancy is strong, forcing the plume to move upward which reduces the recovery of CO_2 in the pull phase. CO_2 flow in the fault gouge develops at a slower rate than in the slip-plane, while CO_2 flow in the damage zone, matrix, and downward is minor. Thermal effects and salt precipitation (not shown here) are minor.

As for active seismic simulation, we used recent theories of seismic modeling of fractures and change in fracture compliance due to CO_2 displacing brine to model a fracture zone with 0% and 50% CO_2 saturation using time-lapse surface seismic and VSP acquisition with 5% random noise added. Both methods had detectable scattering, P-wave and converted S-wave. However, the VSP method had notably larger signal-to-noise ratio due to favorable sensor geometry. These results suggest that the VSP method can be used to characterize a vertical fault/fracture zone 10 m wide at EGS conditions.

Well-logging tools are limited in the EGS environment due to high temperature (T > 175 °C). Induction (HIT) (electrical conductivity) seems to be the most promising measurement, but it will require an open hole environment or fiber-glass casing. Neutron capture (HAPS) monitoring might be feasible for fault gouge (and limited for slip-plane and damage zone), provided enough salinity contrast (or pre-flush with high-salinity brine). The neutron capture method is a shallow measurement (10-25 cm (5-10”) into formation). In general, multiple fractures and wide fault zones will favor imaging by both active seismic and well-logging approaches.

ACKNOWLEDGMENTS

Support for this work was provided by the Office of Energy Efficiency and Renewable Energy, Geothermal Technologies Office, U.S. Department of Energy. Additional support was provided by the Assistant Secretary for Fossil Energy (DOE), Office of Coal and Power Systems, through the National Energy Technology Laboratory (NETL), and by Lawrence Berkeley National Laboratory under Department of Energy Contract No. DE-AC02-05CH11231.

REFERENCES

Coates, R.T. and Schoenberg, M., 1995. Finite-difference modeling of faults and fractures. Geophysics, 60(5), pp.1514-1526.

Corey, A.T., 1954. The interrelation between gas and oil relative permeabilities. Producers monthly, 19(1), pp.38-41.

Faulds, J.E., Coolbaugh, M.F., Benoit, D., Oppliger, G., Perkins, M., Moeck, I. and Drakos, P., 2010. Structural controls of geothermal activity in the northern Hot Springs Mountains, western Nevada: The tale of three geothermal systems (Brady's, Desert Peak, and Desert Queen). Geothermal Resources Council Transactions, 34, pp.675-683.

Genter, A., Evans, K., Cuenot, N., Fritsch, D. and Sanjuan, B., 2010. Contribution of the exploration of deep crystalline fractured reservoir of Soultz to the knowledge of enhanced geothermal systems (EGS). Comptes Rendus Geoscience, 342(7), pp.502-516.

Gudmundsson, A., Fjeldskaar, I. and Brenner, S.L., 2002. Propagation pathways and fluid transport of hydrofractures in jointed and layered rocks in geothermal fields. Journal of Volcanology and Geothermal Research, 116(3), pp.257-278.

Komatitsch, D. and Martin, R., 2007. An unsplit convolutional perfectly matched layer improved at grazing incidence for the seismic wave equation. Geophysics, 72(5), pp.SM155-SM167.

Lutz, S., Moore, J., Jones, C., Suemnicht, G. and Robertson-Tait, A., 2009. Geological and structural relationships in the Desert Peak Geothermal System, Nevada: Implications for EGS development. In Proceedings 34th Workshop on Geothermal Reservoir Engineering.

Madariaga, R., 1976. Dynamics of an expanding circular fault. Bulletin of the Seismological Society of America, 66(3), pp.639-666.

Martin, R., Komatitsch, D. & Ezziani, A., 2008a. An unsplit convolutional perfectly matched layer improved at grazing incidence for seismic wave equation in poroelastic media, Geophysics, 73 (4), T51–T61.

Martin, R., Komatitsch, D. & Gedney, S.D., 2008b. A variational formulation of a stabilized unsplit convolutional perfectly matched layer for the isotropic or anisotropic seismic wave equation, Comput. Modell. Eng. Sci., 37 (3), 274–304.

Martin, R. and Komatitsch, D., 2009. An unsplit convolutional perfectly matched layer technique improved at grazing incidence for the viscoelastic wave equation. Geophysical Journal International, 179(1), pp.333-344.

Nakagawa, S. and Schoenberg, M.A., 2007. Poroelastic modeling of seismic boundary conditions across a fracturea). The Journal of the Acoustical Society of America, 122(2), pp.831-847.

Pan, L., Spycher, N., Doughty, C. and Pruess, K., 2014. ECO2N V. 2.0: A New TOUGH2 Fluid Property Module for Mixtures of Water, NaCl, and CO_2 (No. LBNL-6930E). Ernest Orlando Lawrence Berkeley National Laboratory, Berkeley, CA (US).

Pruess, K., C.M. Oldenburg, and G.J. Moridis. TOUGH2 User's Guide Version 2. E. O. Lawrence Berkeley National Laboratory Report LBNL-43134, 1999; and LBNL-43134 (revised), 2012.

Pruess, K., 2010. Enhanced geothermal systems (EGS) with CO_2 as heat transmission fluid--A scheme for combining recovery of renewable energy with geologic storage of CO_2. Lawrence Berkeley National Laboratory.

Roden, J.A. and Gedney, S.D., 2000. Convolutional PML (CPML): An efficient FDTD implementation of the CFS-PML for arbitrary media. Microwave and optical technology letters, 27(5), pp.334-338.

Snir, M., 1998. MPI--the Complete Reference: The MPI core (Vol. 1). MIT press.

Van Genuchten, M.T., 1980. A closed-form equation for predicting the hydraulic conductivity of unsaturated soils. Soil science society of America journal, 44(5), pp.892-898.

Virieux, J., 1986. P-SV wave propagation in heterogeneous media: Velocity-stress finite-difference method. Geophysics, 51(4), pp.889-901.

Virieux, J. and Madariaga, R., 1982. Dynamic faulting studied by a finite difference method. Bulletin of the Seismological Society of America, 72(2), pp.345-369.